Feasibility of Solar Power for Mars

Joseph Appelbaum and Geoffrey A. Landis
NASA Lewis Research Center
Cleveland, OH

Introduction

NASA, through Project Pathfinder, has put in place an advanced technology program to address future needs of manned space exploration. Included in the missions under study is the establishment of outposts on the surface of Mars. The Surface Power program in Pathfinder is aimed at providing photovoltaic array technology for such an application (as well as for the lunar surface). Figure 1 shows an artist's conception of one such array being deployed by astronauts on the surface of Mars. Another important application is for unmanned precurson missions, such as the photovoltaic-powered airplane shown in figure 2, which will scout landing sites and investigate Mars geology for a 1-2 year mission without landing on the surface (ref. 1).

Detailed information on solar radiation data and the climatic conditions on the Martian surface is necessary to allow accurate estimates of photovoltaic power system size and mass, and as input in system analysis and trade-off studies of technology options. Important information includes the distribution of solar insolation, ambient temperature, albedo, and wind speeds and directions on the surface; all as functions of surface position, season, and time of the day.

Of major concern are the dust storms, which have been observed to occur on local as well as on global scales, and their effect on solar array output. In general, the assumption has been that global storms would reduce solar array output essentially to zero, because the opacity of the atmosphere may rise to values ranging from 3 to 9, depending on the severity of the storm. These high values of opacity may persist for long periods of time such that the requirement for energy storage quickly becomes much too large to be practical. However, as shown in Refs. 2 and 3, there is still an appreciable large diffuse illumination, even at high opacitites, so that solar array operation is still possible.

*This work was done while the authors were National Research Council - NASA Lewis Research Associates.

Calculation of solar radiation incident on the top of Martian atmosphere and on the Martian surface has been previously published (Refs. 4 to 6) taking into account the direct beam component only of the solar radiation. The introduction of the diffuse component in this paper became possible with the normalized net flux. This is described in more detail in reference 2.

As on the planet Earth, the solar radiation on the surface of Mars is composed of two components: the direct ("beam") component and the diffuse component. The direct beam is reduced by scattering and absorption along the path from the top of the Martian atmosphere to the Martian surface. Measurement of the optical depth (Refs. 7 and 8) of the Martian atmosphere allows an estimate of the absorption and scattering out of the beam. These estimates were derived from images taken of the Sun and Phobos with a special diode on the Viking lander cameras.

Earth-terrestrial insolation data are accumulated over many years at different locations around the world and are given as long term average values. The optical depth data for Mars, however, are derived from less than two Mars years. Consequently, the calculated insolation, in the present paper, corresponds to short term data. Furthermore, the measured opacities (optical depth) and the calculated insolation pertain to just two locations on the planet: the Viking lander 1 site, (VL1), located at 22.3° N latitude and 47.9° W longitude; and the Viking lander 2 site, (VL2), located at 47.7° N latitude and 225.7°W longitude. However, the similarity in the properties of the dust suspended above the two landing sites suggests that the sites are representative of ones at other locations, at least, at latitudes not too far from the lander's sites. Data from lander VL1 may be used for latitudes 40°N to 40°S and data from lander VL2 for higher latitudes.

Absorption and scattering by the Martian atmosphere stems mainly from suspended dust particles, the amounts of which vary daily, seasonally, and annually, depending on local and global storm intensities and their duration. Large values of optical depth correspond to global storms, i.e., days with low insolation (dark days).

The albedo of the Martian surface varies in the range of about 0.1 to 0.4. The irradiances derived in the section entitled Solar Radiation correspond to 0.1 albedo, but can be also used for other values of albedo, to the first approximation. In this paper a normalized net solar flux function is introduced from which, together with the variation of the opacities, characteristics of the solar radiation on the Martian surface are calculated. This includes, among others, the diurnal and hourly variation of the global, beam and diffuse radiation on the horizontal surface. The results are presented in a series of figures and tables. The solar radiation data and the procedure presented in this paper can be used for the calculation of any desired solar radiation quantity in engineering design. New information about Mars may be forthcoming in the future from new analysis of previously collected data, from new Earth-based observation, or from future flight missions. The Mars solar radiation data will thus be updated accordingly.

Nomenclature

Radiation values:
G solar irradiance
H daily insolation
I hourly insolation
f(z,τ) diffuse scattering function as a function of sun angle and optical depth
H Mars hour (1/24 sol), equal to 24.65/24 of an actual (terrestrial) hour
hr actual (terrestrial) hour

Subscripts:
b beam (i.e., direct insolation) values
d diffuse values
h values for a fixed horizontal surface
o values on top of Mars atmosphere

Other values:
e orbital eccentricity = 0.093377
Ls areocentric longitude (position of Mars in orbit)
m(z) air mass as a function of solar zenith angle
r instantaneous Sun-Mars distance in astronomical units (AU).
S solar constant = 1371 W/m^2 at the mean Sun-Earth distance of 1 AU.
T Mars solar time
T_d Mars daylight hours
z zenith angle of the sun
δ declination angle
δ_o axial tilt of Mars = 24.936°
τ optical depth (opacity) of the atmosphere
ϕ latitude
ω hour angle, measured at 15° per (Mars) hour from solar noon.

Optical Depth

The most direct and probably most reliable estimates of opacity are those derived from Viking lander imaging of the Sun. Figures 3 and 4 show the seasonal variation of the normal-incidence of the optical depth at the Viking lander locations VL1 and VL2, respectively. The season is indicated by the the value of Ls, areocentric longitude of the Sun, measured in the orbital plane of the planet from its vernal equinox (Ls = 0°). The optical depth values were derived from references by Pollack (Refs. 7 and 8) and Zurek (Ref. 9) and discretized for each 5° of Ls value. The optical depth is assumed to remain constant throughout the day. Opacities are minimum during the northern spring (Ls = 0° to 90°) and summer (Ls = 90° to 180°), and maximum during southern spring (Ls = 180° to 270°) and summer (Ls = 270° to 360°), the seasons during which most local and major dust storms occur. When dust storms

are not present, the optical depth is typically about 0.5, corresponding to a direct-beam solar intensity (at zenith angle of 90°) of exp(-0.5) = 61% of I_o. Two global dust storms occurred during the periods of each observation as indicated by the high values of the optical depth (they are lower bound values).

Mars has seasons comparable to those of Earth. However, the seasons are on the average about twice as long as on the Earth, corresponding to the greater length of the Martian year (Table I). Furthermore, they are distinctly unequal in duration as a result of the appreciable eccentricity of the Martian orbit. For that reason, the Martian year is not divided into months. Table I gives the duration of the Martian seasons in terrestrial and Martian days (a Martian day, or "sol", = 24.65 hr). Areocentric longitudes Ls = 0° and 180° correspond to the spring and fall equinox for the northern hemisphere, respectively, and Ls = 90° and 270° correspond to northern and southern summer solstices, respectively.

Global and Local Dust Storms

The intensity of Martian global and local dust storms is defined in terms of the atmospheric opacity created by the dust raised. Global dust storms obscure planetary-scale sections of the Martian surface for many martian days (sols). Local dust srorms are less intense, and form and dissipate in a few days or less. From a photovoltaic system design point of view, the intensity, frequency, and duration of these storms may be viewed as "partially cloudy" and "cloudy" days, for which additional capacity and possibly energy storage may be required. Characeristics of global and local dust storms are listed below.

Global Dust Storms

(1) One, or occasionally two, global dust storms of planetary scale may occur each Martian year. The duration may vary from 35 to 70 days or more. Although global dust storms may not occur every year, their occurrance is fairly frequent.

(2) The global dust storms occur near perihelion, i.e., southern hemisphere spring and summer, when insolation is maximum in the southern mid-latitudes where such storms typically originate.

(3) The first global dust storm observed by Viking (1977) spread from a latitude of 40°S to a latitude of 48°N in about 5 to 6 days.

(4) The atmospheric opacity during a global dust story is typically greater than 1.

Local Dust Storms

(1) Local dust storms occur at almost all latitudes and throughout the year. However, they have been observed to occur most frequently in the latitude 10° to

20°N and 20° to 40°S, with more dust clouds seen in the south than in the north, the majority of which occurred during the southern spring.

(2) Based on Viking orbiter observations, it is estimated that approximately 100 local storms occur in a given Martian year.

(3) Local dust storms last a few days.

(4) Atmospheric opacity during a local dust storm may be assumed to be about 1.

Solar Radiation at the Top of the Mars Atmosphere

The variation of the solar radiation at the top of the Mars atmosphere is governed by the location of Mars in its orbit and by the solar zenith angle. The sun-Mars distance is (ref. 10):

$$r = a \frac{(1 - e^2)}{[1 + e\ cos(Ls - 248°)]} \tag{1}$$

where 248° is the areocentric longitude of the perihelion of the orbit. The sun-Mars mean distance a is 1.52369 AU (Astronomical units), thus, the mean irradiance at the top of the Martian atmosphere is $1371/1.52369^2 = 590$ W/m^2. The irradiance thus varies with orbital position as:

$$G_{ob} = 590 \frac{[1 + e\ cos(Ls - 248°)]^2}{(1 - e^2)} \text{ W/m}^2 \tag{2}.$$

This is the solar intensity which would be received, for example, by a Mars orbiter.

The solar zenith angle is a function of the solar declination angle, given by:

$$Cos(z) = sin\phi\ sin\delta + cos\phi\ cos\delta\ cos\omega \tag{3}$$

where the solar declination angle is:

$$sin(\delta) = sin\delta_o sin Ls \tag{4}$$

The four seasons pertain here to the northern hemisphere; the seasons are reversed for the southern hemisphere.

The ratio of Mars to Earth length of day is 24.65/24. It is convenient, for calculation purposes, to define a Mars hour, H, 2.7% longer than a terrestrial hour, by dividing the Martian day (sol) into 24 Martian hours. The final solar radiation results expressed in terms of Mars hours can then be multiplied by 1.027 to give results in actual (terrestrial) time.

Examples of the solar radiation calculation procedure and results shown pertain to five example days at Viking Lander location VL1 at $\phi = 22.3°$N. Areocentric longitude Ls=69° corresponds to aphelion, the lowest exoatmospheric irradiance; Ls=249° to perihelion, the highest exoatmospheric irradiance; Ls=153° to the mean radiation of 590 W/m^2; Ls=120° corresponds to the lowest observed atmospheric opacity of 0.4, and Ls=299° to the highest opacity of 3.25.

For a given Ls and latitude ϕ, one can calculate the zenith angle z as a function of time using equations (3) and (4). The direct beam irradiance on a horizontal surface is then determined by multiplying the direct irradiance from equation (2) by the cosine of the zenith angle. The number of daylight hours is (from ref. 11):

$$T_d = 1.027 \cdot \frac{12}{15} \, cos^{-1}(-tan \, \phi \, tan \, \delta) \tag{5}.$$

Table II gives the hourly beam insolation I_{obh} and the daily beam insolation H_{obh} on a horizontal surface at the top of the atmosphere. To obtain terrestrial watt-hours, one needs to multiply the values in Table II by 1.027.

Solar Radiation on the Surface of Mars

The variation of the solar radiation on the Martian surface is governed by three factors: (1) the Mars-sun distance, (2) the solar zenith angle, and (3) the opacity of the atmosphere. The global solar radiance is composed of direct beam and the diffuse components. The direct beam irradiance normal to the incident rays, G_b, is related to the optical depth of the intervening suspended dust by (Beer's law):

$$G_b = G_{ob} exp[-\tau \, m(z)] \tag{6}$$

where m(z) is the air mass determined by the zenith angle z, and can be approximated, for zenith angles up to about 80°, by:

$$m(z) \approx \frac{1}{cos(z)} \tag{7}.$$

The net solar flux integrated over the solar spectrum on the Martian surface was calculated by Pollack (Ref. 12) based on multiple wavelength and multiple scattering of the solar radiation. Derived data from this calculation are shown in Table III by the normalized net flux function $f(z, \tau)$ where the parameters are the zenith angle z and the optical depth τ. This table pertains to an albedo of 0.1. Using this data we calculated the global solar irradiance. We assumed that the diffuse irradiance is obtained by subtracting the direct beam from the global irradiance. The solar irradiance components, on a horizontal Martian surface, is the sum of the direct beam and the diffuse components:

$$G_h = G_{bh} + G_{dh} \tag{8}.$$

The diffuse irradiance of the Martian atmosphere may be a result of a different mechanism than that for the Earth atmosphere, nevertheless, we can apply Eq. (7) as for Earth-terrestrial calculations. The global irradiance G_h on a horizontal surface is given by:

$$G_h = G_{ob} cos(z) \frac{f(z,\tau)}{0.9} \tag{9}.$$

The factor 0.9 comes from the expression (1-albedo) in the denominator assuming albedo of 0.1. This accounts for sunlight reflected from the ground and backscattered by atmospheric dust back to the solar array. An albedo value of 0.1 is conservative. The actual Mars albedo can be as high as 0.4. To first order, higher surface albedo can be taken into account by replacing the 0.9 in (9) by (1-albedo).

The direct beam irradiance G_{bh} on a horizontal surface is obtained by:

$$G_{bh} = G_{ob}\ cos(z)\ exp[\frac{-\tau}{cos(z)}] \tag{10}.$$

The diffuse irradiance on a horizontal surfaces is obtained from Eqs. (7) to (9). The irradiances were calculated based on Table III data and the mean irradiance of 590 W/m^2. The variation of the global irradiance on a horizontal Martian surface, G_h, Eq. (8), is shown in Fig. 6 as a function of the optical depth τ and zenith angle z.. The direct beam irradiance on a horizontal surface G_{bh} is obtained using Eq. (9) and is shown in Fig. 7. The direct beam irradiance shows a sharp decrease with increasing optical depth, and a relatively moderate decrease with increasing zenith angle. The diffuse irradiance on a horizontal surface G_{dh} is shown in fig. 8. The diffuse irradiance shows a sliding maximum with the variation of the zenith angle.

The solar radiation (global, direct beam and diffuse) variation (diurnal, hourly and daily) can be calculated based on the preceeding equations and the $f(z,\tau)$ data of Table III. The following examples pertain again to the Viking lander VL1 location and the five example days at areocentric longitudes Ls = 69°, 120°, 153°, 249°, and 299°, representative of the the range of martian conditions. Daily solar insolation are also given for Ls = 0°, 30°, 60°, 90°, 150°, 180°, 210°, 240°, 300°, and 330°. For a given Ls and ϕ, one can calculate the variation of the zenith angle z as function of the Mars solar time T using Eqs. (3) and (4). Referring to Fig. 3 for the given Ls, the optical depth τ is determined; with Table III and Eqs. (6) to (10) one can calculate the solar radiation variation for the given day. The results are shown in Figs. 9 to 11. (Because of symmetry around solar noon, the graphs show the forenoon or afternoon

variation.) The figures show clearly that for higher opacities, the diffuse component dominates the solar radiation.

The total (global, direct beam and diffuse) energy on a horizontal surface can be calculated based on Figs. 9 to 11 by integrating hourly areas. The direct beam insolation, for a desired period of time, can be also calculated by:

$$I_{bh} = \frac{12^*}{\pi} G_{ob} \int_{\omega_1}^{\omega_2} [sin\phi\ sin\delta + cos\phi\ cos\delta\ cos\omega]\ exp[\frac{-\tau}{(sin\phi sin\delta + cos\phi cos\delta cos\omega)}]\ d\omega \quad (11).$$

*Replace the 12 by 12.325 in Eq. (11) to get the insolation with reference to actual (terrestrial) time.

Tables IV to VI give the hourly global I_h, direct beam I_{bh} and diffuse I_{dh} insolation as well as the daily global H_h, direct beam H_{bh} and diffuse H_{dh} insolation. Included in the tables are also the number of Martian daylight hours and the daily mean irradiance. For a day with a relative high opacity (Ls = 299°), the daily mean global irradiance is still appreciable and is about 30 percent of that in a clear day. The percentage of diffuse and direct beam insolation for the five analyzed Ls days is shown in Fig. 12. The daily global insolation on a horizontal surface on Mars is shown in Fig. 13 for twelve areocentric longitudes covering a Martian year. Using the procedure outlined, one can calculate the variation of the solar radiation for any desired day to use for any engineering system design.

Temperature

The ambient air temperature at the Viking lander's locations was measured for more than two Martian years at the height of 1.6 m above the ground. The ambient temperature sensors consists of chromel-constantan thermocouples. Again, these are short term data and pertain to the two Viking locations. While the array operating temperature will not, in general, be the same as the local air temperature, measured air temperature is needed as one factor needed to compute the array operating temperature

Mars temperature data was information was supplied to us by Tillman (ref. 13). Figure 14 shows the variation of the ambient temperature at Viking lander VL1 for part of the first year after landing. The top time coordinate (abscissa) has units of sol number, the number of Martian solar days from touchdown on sol 0 (1 sol = 24.65 hr). The bottom abscissa is the seasonal date Ls. The temperature variation over the course of a day is shown in more detail for sols 191 and 192 (autumn) in figure 15. The figure shows a quite significant large diurnal ambient temperature variation. Figure 16 shows the ambient temperature at Viking lander VL2 for the first year after landing. During dust storm events, the Martian atmosphere is strongly

heated up by absorption of solar radiation due to the suspended dust. As a result, the maximum ambient temperature at the surface decreases significantly while the minimum increases, especially during the more intense 1977 B storm. The diurnal ambient temperature variation for sols 285 and 286 at the time of 1977 B global storm is shown in Fig. 17. The variation in temperature, 16°C, is rather small. For the less intense 1977 A global storm, the diurnal temperature variation was larger (28°C), and for a local storm, the diurnal ambient temperature variation is still larger (38°C).

Wind

An array deployed on Mars will have to withstand wind loads. Surface wind velocities were measured at the VL-2 site. The average windspeed is about 2 m/sec. 90% of the time the wind was below 5 m/sec; 99% of the time below about 15 m/sec. For some applications it may be a viable design strategy to retract the array if windspeeds reach higher values. Less than 0.01% of the time the winds reached 25-30 m/sec. During dust storms up to 32 m/sec has been observed.

Due to the very low air density, the actual pressures produced by the wind are not very high. The effect is roughly that of a terrestrial wind of 1/7th the velocity.

Atmospheric pressure varies with season and temperature. At a typical pressure of 8 mb and temperature of 200°K, the maximum wind velocity of 30 m/sec produces a dynamic pressure of 10 nt/m^2, similar to that of a 4 m/sec (9 MPH) wind on Earth.

The array surface will have to resist abrasion by wind-blown sand and dust. Since the atmospheric density is so low, sand should not be lifted more than a few centimeters above the surface. Dust can be blown quite high in the atmosphere; however, since typical dust seems to consist of silicate particles with mean radius of 1 to 2 micron, abrasion due to dust is not expected to be a significant difficulty. The question of whether the array can be designed so that settling dust will be cleared from the array surface by wind is currently being addressed in wind tunnel studies (ref. 14); preliminary results seem to indicate that this will be the case if the array surface is tilted from the horizontal.

Conclusions

Effective design and utilization of solar energy depend to a large extent on adequate knowledge of solar radiation characteristics in the region of solar energy system operation. The two major climatic components needed for photovoltaic system design are the distributions of solar insolation and ambient temperature. These distributions for the Martian climate are given in the paper at the two Viking lander locations but can also be used, to the first approximation, for other latitudes. One of the most important results of this study is that there is a large diffuse component of the insolation, even at high optical depth, so that solar energy system operation is still

possible. If the power system is to continue to generate power even on high optical opacity (i.e., dusty atmosphere) days, it is thus important that the photovoltaic system be designed to collect diffuse irradiance as well as direct. In absence of long term insolation and temperature data for Mars, the data presented in this paper can be used until updated data are available. The ambient temperature data are given as measured directly by the temperature sensor; the insolation data (global, direct beam, and diffuse) are calculated from optical depth measurements of the atmosphere. Additional insolation data, such as daily insolations, can be further derived based on Table 1 and the expressions above and in reference 3.

Acknowledgement

We are very grateful to James B. Pollack from the Space Science Division, NASA Ames Research Center for supplying us with the $f(z,\tau)$ table; to James E. Tillman from the Department of Atmospheric Sciences, University of Washington for supplying the ambient temperature distribution graphs; and for their informative discussions.

References

[1.] A.J. Colozza, *to be published, 26th AIAA/SAE/ASME/ASEE Joint Propulsion Conf.,* Orlando, FL, 16-18 July 1990.

[2.] J. Appelbaum and D. J. Flood, Space Power, **8**, No. 3, 307, 1989.

[3.] J. Appelbaum and D. J. Flood, NASA Technical Memorandum TM-102299, 1989 (to be published, Solar Energy, 1990).

[4.] J. S. Levine, D. R. Kramer and W. R. Kuhn, ICARUS, **31**, 136, 1977.

[5.] E. Van Hemelrijk, Earth, Moon, and Planets, **33**, 157, 1985.

[6.] E. Van Hemelrijk, Earth, Moon, and Planets, **38**, 209, 1987.

[7.] J. B. Pollack, et al., Journal of Geophysical Research, **82**, 4479, 1977.

[8.] J. B. Pollack, et al., Journal of Geophysical Research, **84 B6**, 2929, 1979.

[9.] R. W. Zurek, ICARUS, **50**, 288, 1982.

[10.] E. V. P. Smith and K. C. Jacobs, *Introductory Astronomy and Astrophysics,* W.B. Saunders Co., 1973.

[11.] J. A. Duffie, W. A. Beckman, Solar Engineering of Thermal Processes, Wiley, 1980.

[12.] J. B. Pollack, R. M. Harberle, J. Schaeffer, H. Lee, Journal of Geophysical Research (in press).

[13.] J. E. Tillman, Director and N. C. Johnson, Viking Computer Facility, Department of Atmospheric Sciences, University of Washington, Seattle, Washington, private communication.

[14.] J.R. Gaier, M.E. Perez-Davis, and M. Marabito, NASA Technical Memorandum TM-102507, Feb. 1990 (in press).

TABLE I. - MARS SEASONAL DURATION

Areocentric longitude of the sun, L_s	Season		Duration of the season Mars	
	Northern hemisphere	Southern hemisphere	Martian days	Terrestrial days
0 to 90°	Spring	Autumn	194	199
90 to 180°	Summer	Winter	178	183
180 to 270°	Autumn	Spring	143	147
270 to 360° or 0°	Winter	Summer	154	158
			669	687

TABLE II. - HOURLY AND DAILY BEAM INSOLATION ON A HORIZONTAL SURFACE AT TOP OF MARS ATMOSPHERE

[VL1: ϕ = 22.3°N]

Hourly* I_{obh} (Whr/m^2-hr) for hours ending at:								Daily* H_{obh}, Whr/m^2-day
Day-L_s	13:00	14:00	15:00	16:00	17:00	18:00	19:00	
69°	488	460	405	328	234	128	25	4136
120°	528	497	437	353	249	134	23	4442
153°	572	536	467	368	247	113	7	4620
249°	496	455	376	263	126	8	--	3449
299°	478	439	364	257	127	10	--	3350

*Multiply by 24.65/24 to obtain actual (terrestrial) Whr/m^2

TABLE III. - NORMALIZED NET FLUX FUNCTION $f(z,\tau)$ AT THE MARTIAN SURFACE

Optical depth	Zenith angle Z, deg									
τ	0	10	20	30	40	50	60	70	80	85
0.1	0.885	0.883	0.882	0.880	0.876	0.870	0.857	0.830	0.755	0.635
0.2	.866	.865	.860	.858	.851	.836	.813	.758	.640	.470
0.3	.847	.846	.841	.836	.826	.806	.774	.708	.562	.412
0.4	.828	.827	.821	.815	.802	.778	.740	.667	.502	.373
0.5	.810	.810	.802	.796	.778	.752	.708	.628	.452	.342
0.6	.793	.791	.785	.775	.755	.725	.677	.593	.414	.318
0.7	.776	.773	.766	.755	.733	.700	.646	.555	.383	.298
0.8	.760	.756	.750	.736	.710	.675	.616	.520	.360	.280
0.9	.745	.740	.733	.717	.690	.650	.587	.487	.336	.264
1.0	.732	.725	.717	.700	.670	.628	.560	.455	.317	.252
1.1	.713	.709	.700	.682	.651	.604	.539	.433	.300	.239
1.2	.697	.692	.683	.662	.632	.585	.518	.413	.288	.230
1.3	.682	.677	.667	.646	.613	.567	.498	.394	.273	.220
1.4	.666	.661	.650	.629	.596	.546	.478	.379	.262	.210
1.5	.651	.646	.633	.612	.580	.530	.460	.362	.251	.202
1.6	.637	.630	.618	.597	.563	.512	.441	.348	.240	.195
1.7	.622	.615	.601	.581	.546	.494	.424	.332	.232	.188
1.8	.609	.600	.586	.568	.531	.480	.408	.318	.224	.181
1.9	.596	.587	.571	.551	.514	.464	.393	.304	.217	.176
2.0	.582	.573	.558	.537	.500	.448	.378	.293	.208	.170
2.25	.552	.542	.522	.501	.462	.410	.343	.265	.190	.156
2.50	.518	.509	.492	.469	.430	.378	.316	.242	.174	.145
2.75	.486	.478	.462	.440	.401	.353	.293	.224	.158	.136
3.00	.460	.450	.434	.414	.376	.330	.273	.206	.150	.128
3.25	.434	.424	.410	.390	.354	.308	.254	.193	.140	.120
3.50	.411	.400	.387	.367	.333	.290	.240	.180	.132	.110
4.00	.370	.360	.347	.330	.296	.258	.212	.160	.118	.100
5.00	.294	.286	.275	.258	.230	.203	.166	.130	.094	.080
6.00	.228	.223	.215	.200	.178	.153	.130	.103	.080	.068

TABLE IV. - HOURLY AND DAILY GLOBAL INSOLATION ON A HORIZONTAL SURFACE AT MARS SURFACE

[VL1: ϕ = 22.3°N]

Hourly global insolation* I_h (Whr/m^2-hr) for hours ending at:									Daily global insolation,* H_h, Whr/m^{2}day	Daylight hours* T_d, hr	Daily mean global irradiance, W/m^2
Day-L_s	τ	13:00	14:00	15:00	16:00	17:00	18:00	19:00			
69°	0.65	420	390	338	263	170	78	11	3340	13.34	250
120°	.40	477	446	387	306	201	98	15	3860	13.24	292
153°	.50	508	471	399	302	185	73	3	3882	12.62	308
249°	1.40	307	270	204	122	45	2	--	1900	10.66	178
299°	3.25	170	149	107	61	24	1	--	1024	10.75	95

*Multiply by 24.65/24 to obtain actual (terrestrial) Whr/m^2 or hours

TABLE V. - HOURLY AND DAILY BEAM INSOLATION ON A HORIZONTAL SURFACE AT MARS SURFACE

[VL1: ϕ = 22.3°N]

Hourly beam insolation* I_{bh} (Whr/m^2-hr) for hours ending at:									Daily beam insolation*, H_{bh}, Whr/m^{2}day	Daylight hours* T_d, hr	Daily mean beam irradiance, W/m^2
Day-L_s	τ	13:00	14:00	15:00	16:00	17:00	18:00	19:00			
69°	0.65	252	230	186	128	67	20	3	1768	13.34	133
120°	.40	352	322	265	190	103	33	2	2534	13.24	191
153°	.50	345	310	244	163	77	15	--	2308	12.62	183
249°	1.40	69	50	26	10	2	--	--	314	10.66	29
299°	3.25	3	2	1	---	--	--	--	12	10.75	1

*Multiply by 24.65/24 to obtain actual (terrestrial) Whr/m^2 or hours

TABLE VI. - HOURLY AND DAILY DIFFUSE INSOLATION ON A HORIZONTAL SURFACE AT MARS SURFACE

[VL1: = 22.3°N]

Hourly diffuse insolation* I_{dh} (Whr/m^2-hr) for hours ending at:									Daily diffuse insolation,* H_{dh}, Whr/m^{2}day	Daylight hours* T_d, hr	Daily mean diffuse irradiance, W/m^2
Day-L_s	τ	13:00	14:00	15:00	16:00	17:00	18:00	19:00			
69°	0.65	168	160	152	135	103	58	10	1572	13.34	118
120°	.40	125	124	122	116	98	65	13	1326	13.24	100
153°	.50	163	161	155	139	108	58	3	1574	12.62	125
249°	1.40	238	220	178	112	43	2	--	1586	10.66	149
299°	3.25	167	147	106	61	24	1	--	1012	10.75	94

*Multiply by 24.65/24 to obtain actual (terrestrial) Whr/m^2 or hours

Figure 1: artist's conception of a roll-out solar array being deployed by astronauts on Mars.

Figure 2: artist's conception of a photovoltaic-powered unmanned Mars airplane.

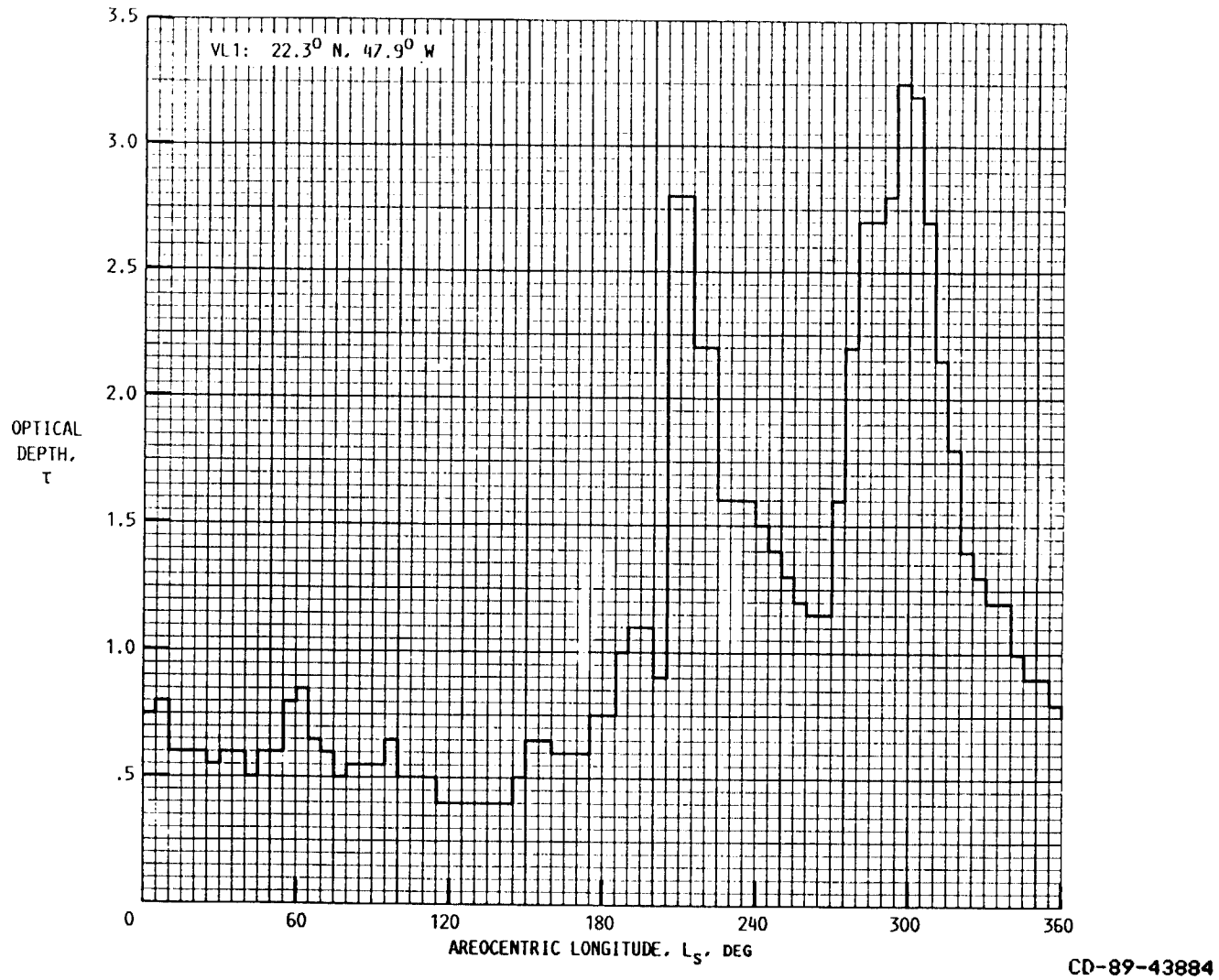

Figure 3: seasonal variation of the normal-incidence of the optical depth at the Viking lander location VL1 [From Pollack (Refs. 7 and 8) and Zurek (Ref. 9)].

Figures 4: seasonal variation of the normal-incidence of the optical depth at the Viking lander location VL2 [From Pollack (Refs. 7 and 8) and Zurek (Ref. 9)].

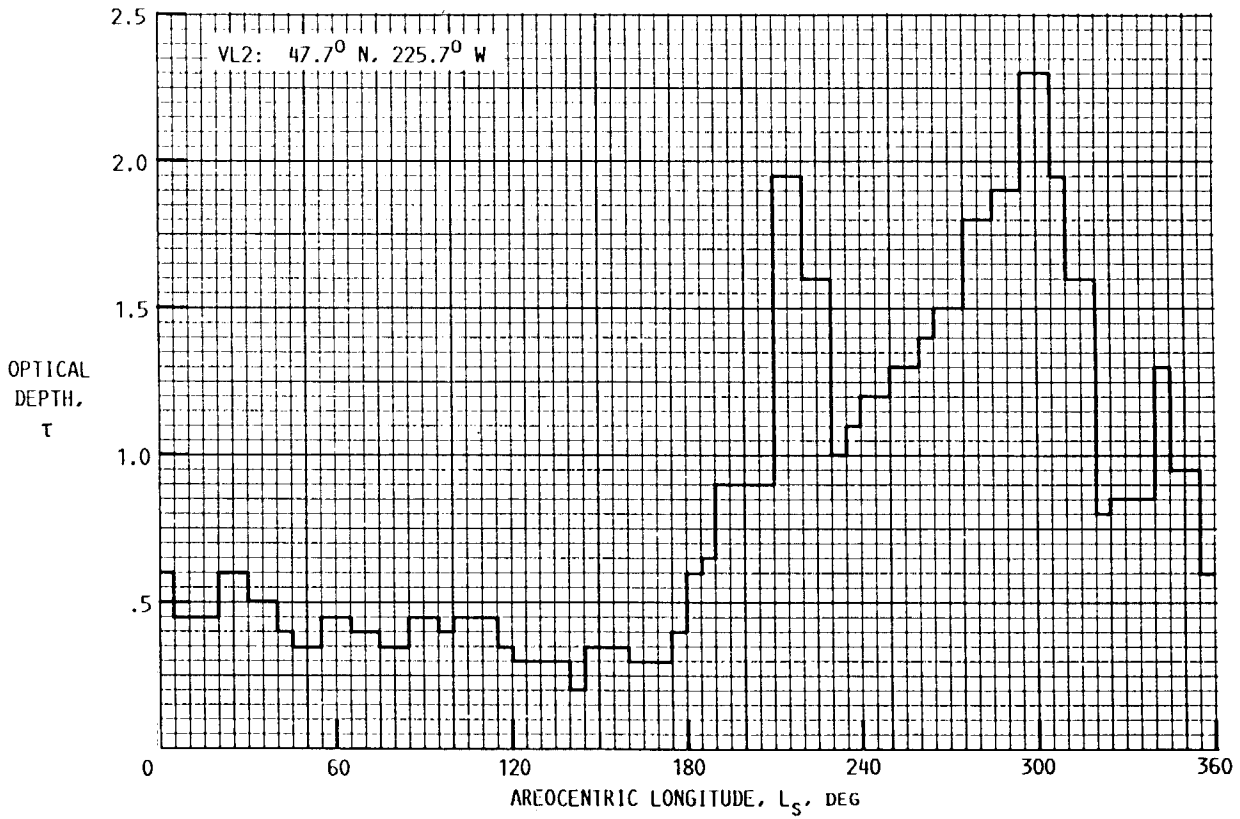

CD-89-43885

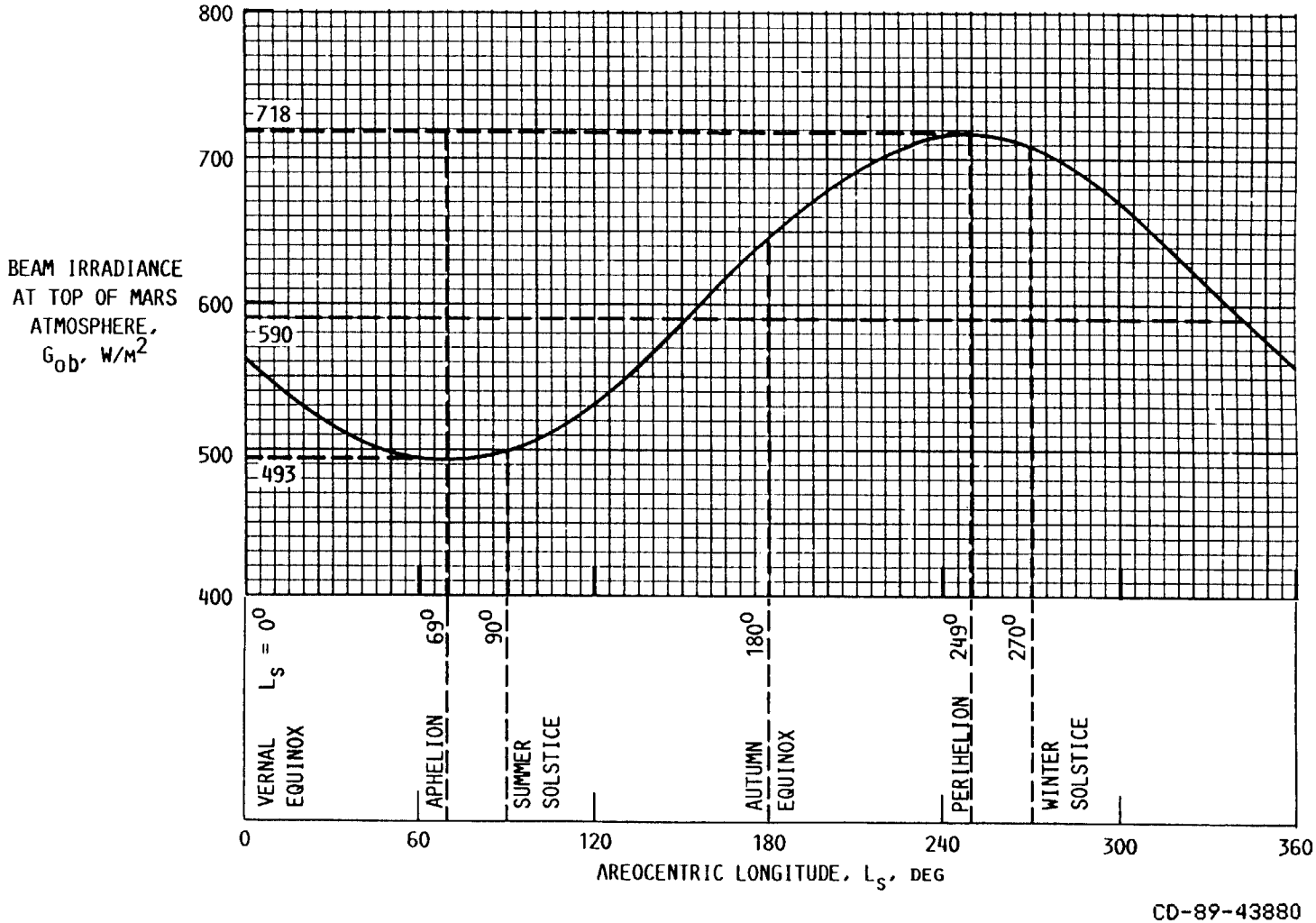

Figure 5: Solar irradiance above the Mars atmosphere as a function of position of Mars in orbit.

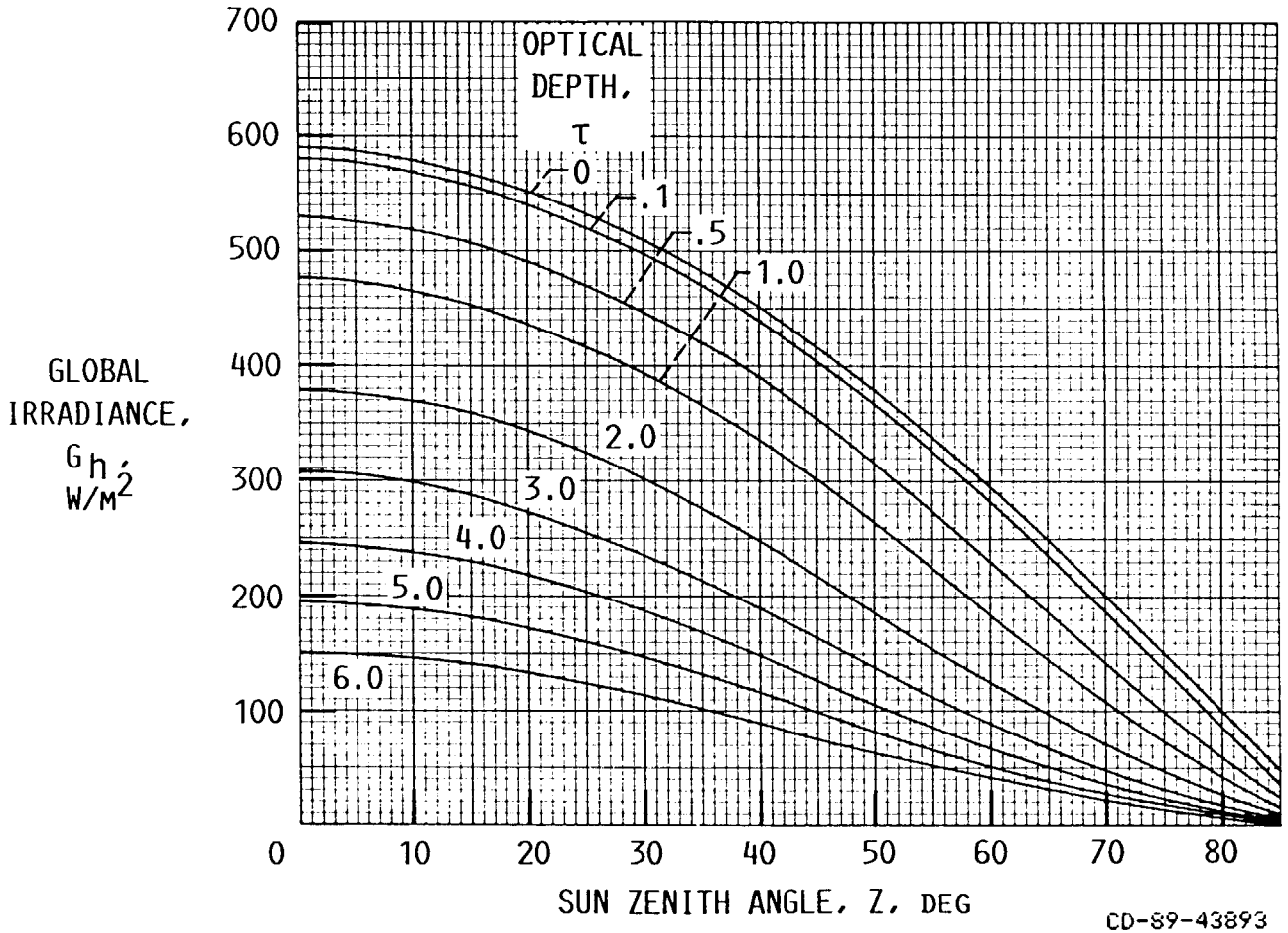

Figure 6: the variation of the global irradiance G_h on a horizontal Martian surface as a function of the optical depth τ and zenith angle z.

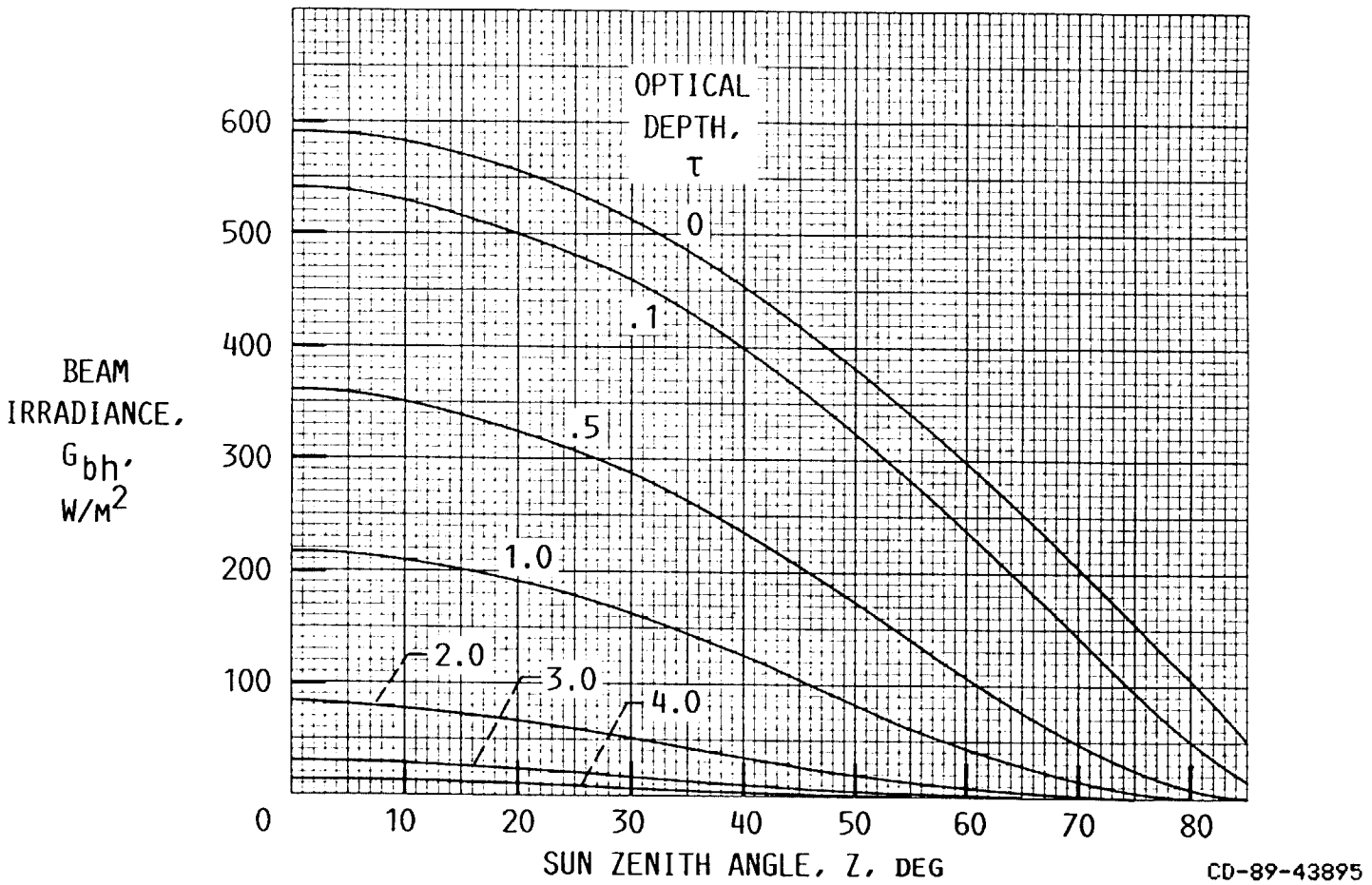

Figure 7: the direct beam irradiance G_{bh} on a horizontal Martian surface as a function of the optical depth τ and zenith angle z.

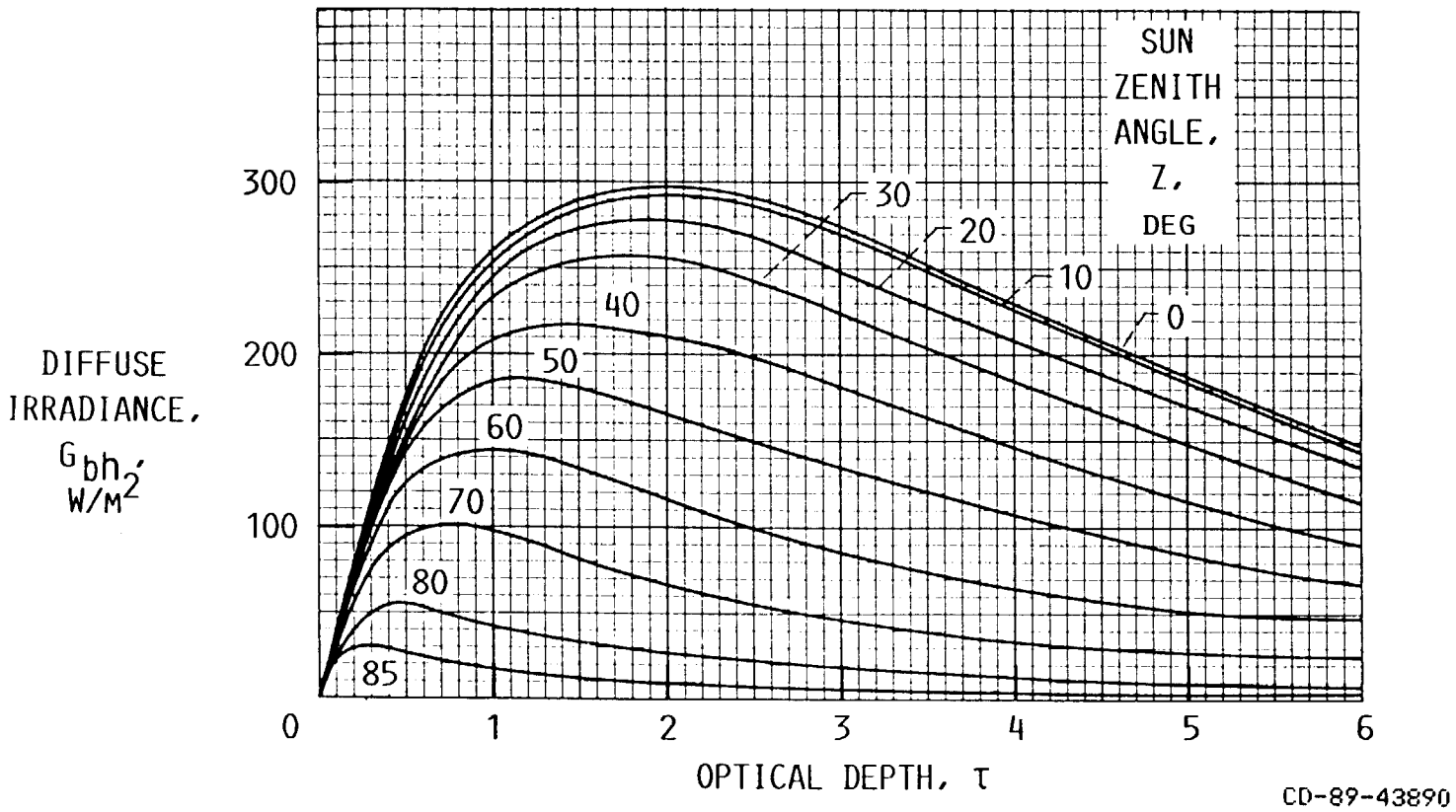

Figure 8: the diffuse irradiance G_{dh} on a horizontal Martian surface as a function of the optical depth τ and zenith angle z.

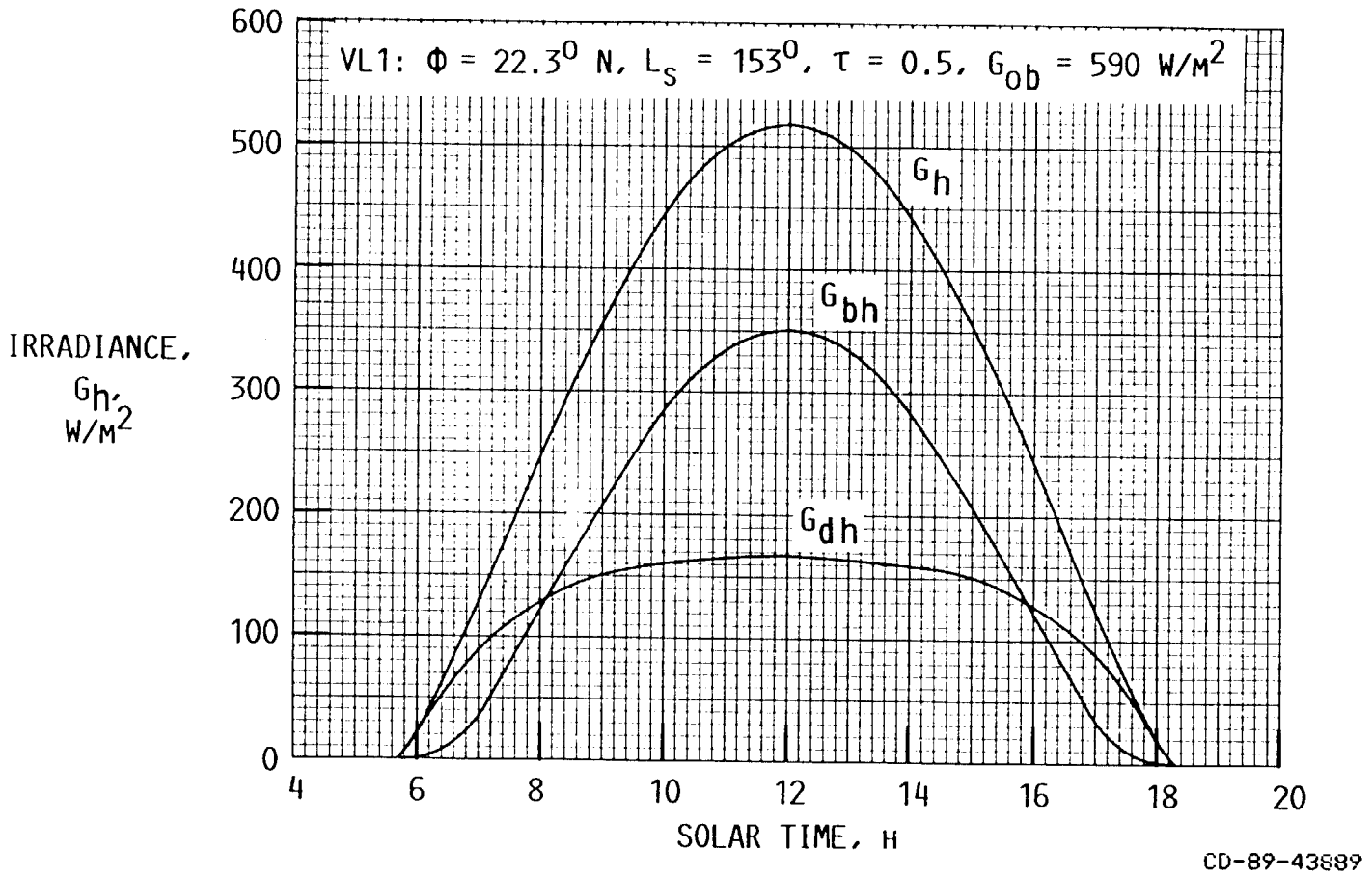

Figures 9-11: the solar radiation variation for several particular days.

Figure 9

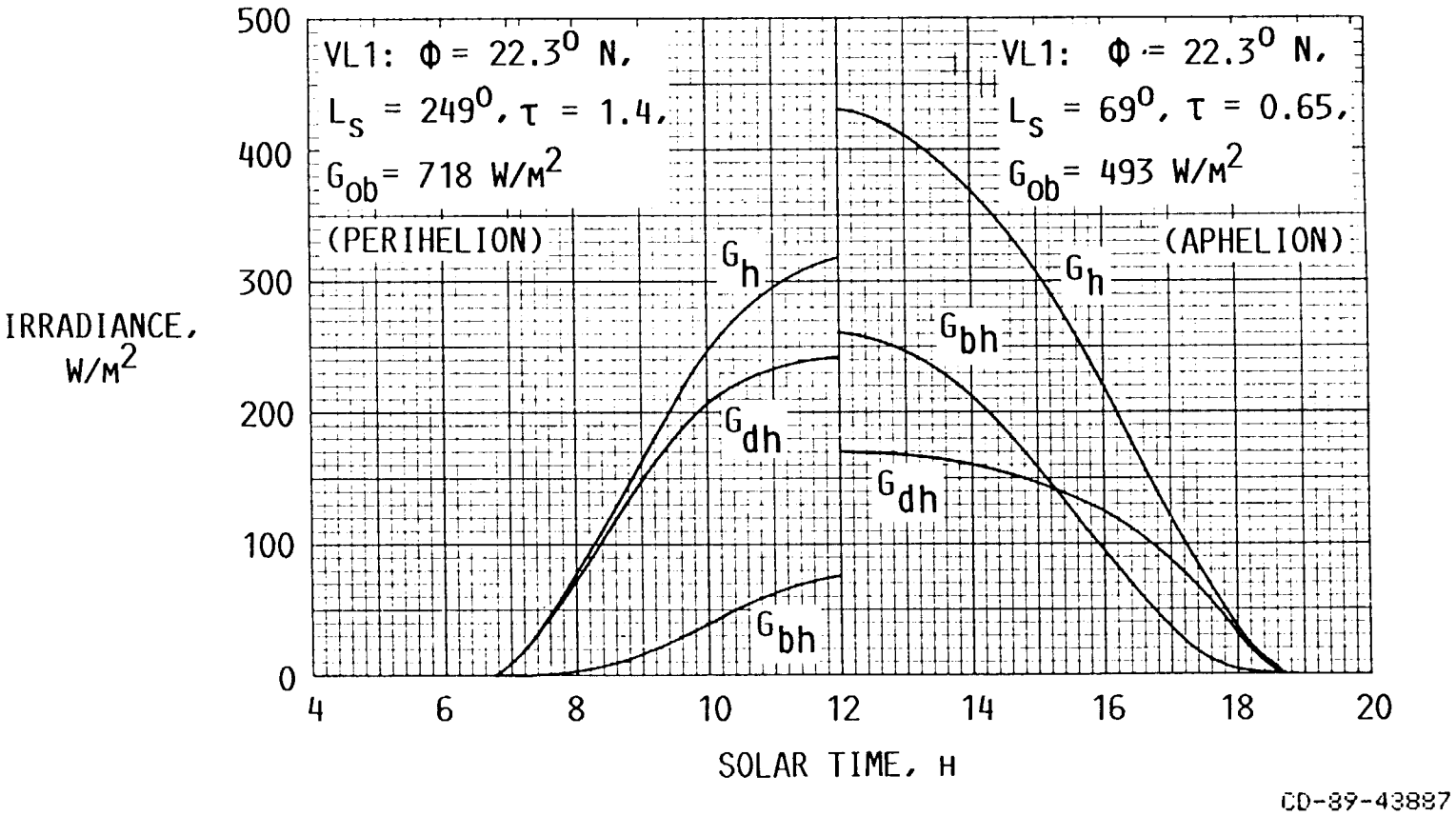
VL1: Φ = 22.3° N,
Ls = 249°, τ = 1.4,
Gob = 718 W/m2
(PERIHELION)
VL1: Φ = 22.3° N,
Ls = 69°, τ = 0.65,
Gob = 493 W/m2
(APHELION)
Gh
Gbh
Gdh
IRRADIANCE, W/m2
SOLAR TIME, H
CD-89-43887

Figure 10

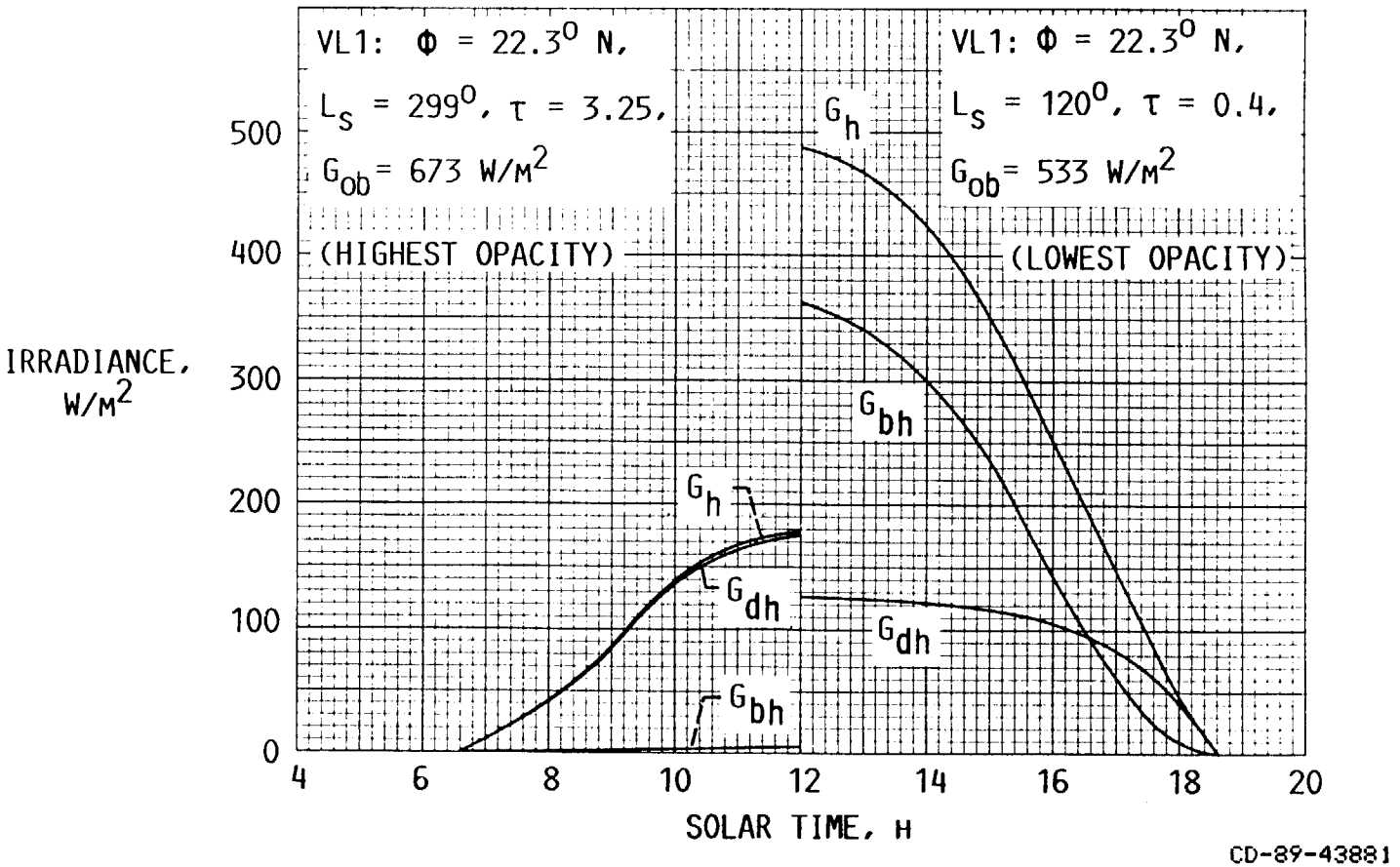
VL1: Φ = 22.3° N,
Ls = 299°, τ = 3.25,
Gob = 673 W/m2
(HIGHEST OPACITY)
VL1: Φ = 22.3° N,
Ls = 120°, τ = 0.4,
Gob = 533 W/m2
(LOWEST OPACITY)
Gh
Gbh
Gh
Gdh
Gdh
Gbh
IRRADIANCE, W/m2
0
100
200
300
400
500
4
6
8
10
12
14
16
18
20
SOLAR TIME, H
CD-89-43881

Figure 11

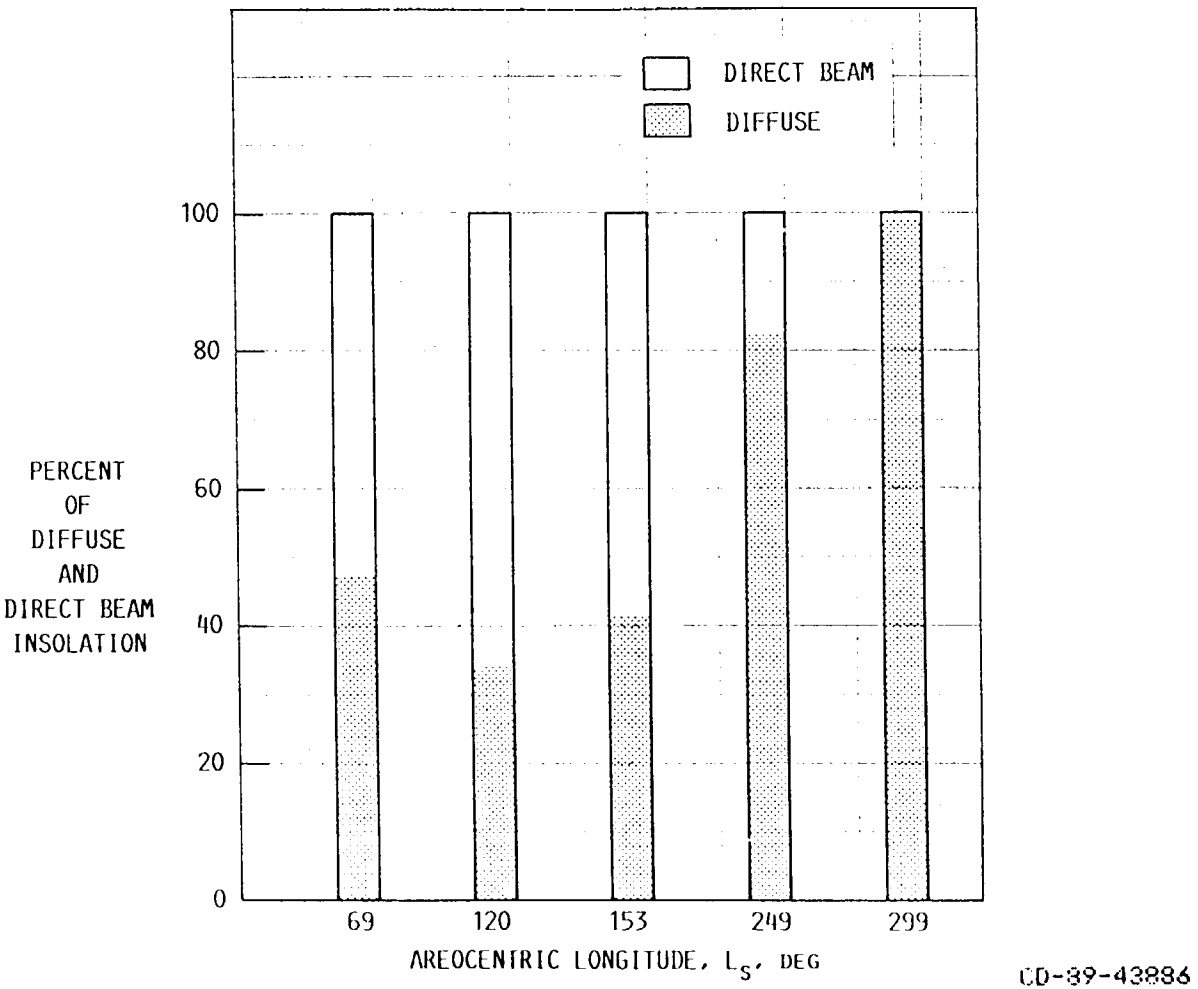

Figure 12: the percentage of diffuse and direct beam insolation for the five analyzed Ls days.

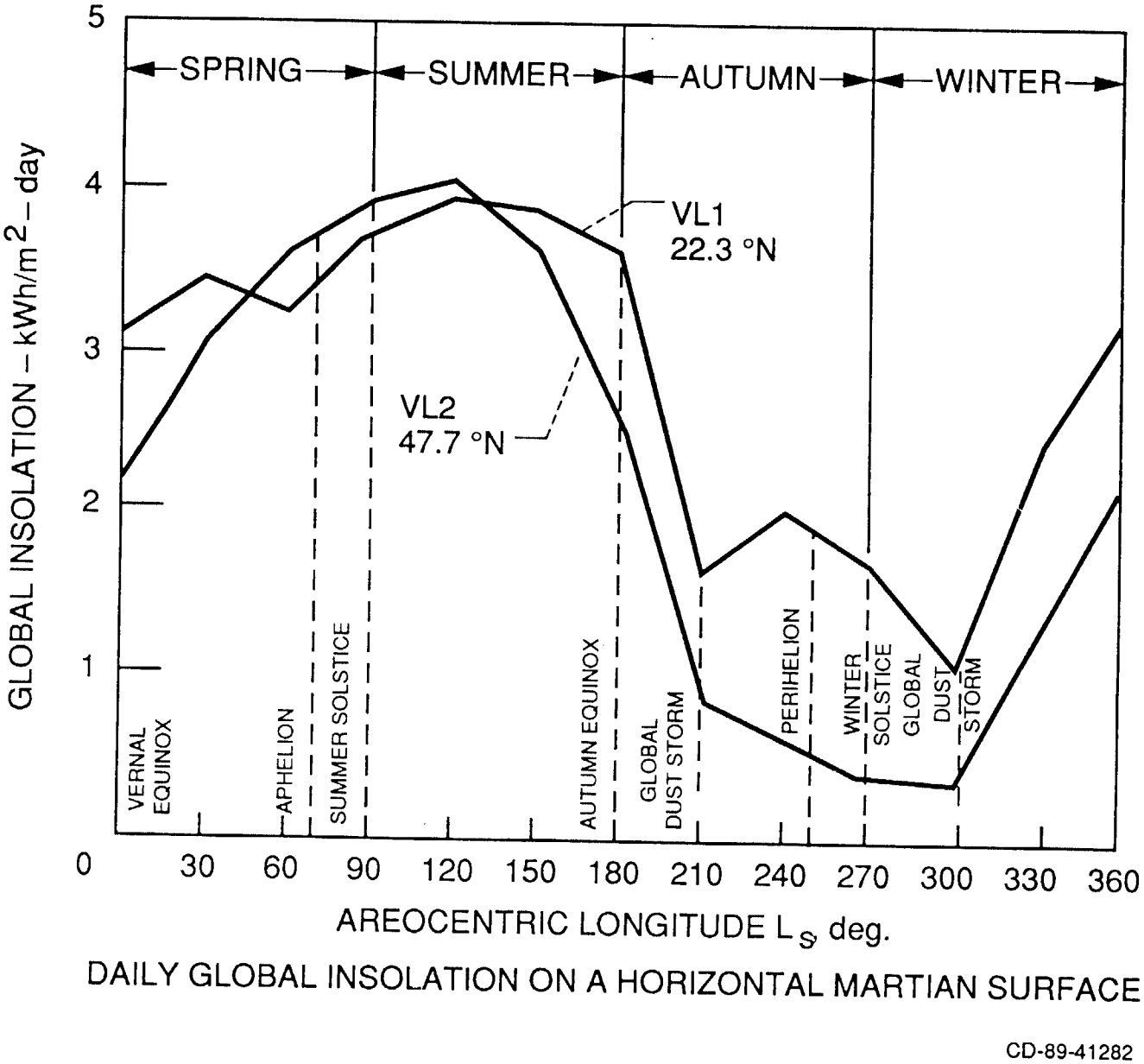

Figure 13: the daily global insolation on a horizontal surface on Mars for twelve areocentric longitudes covering a Martian year.

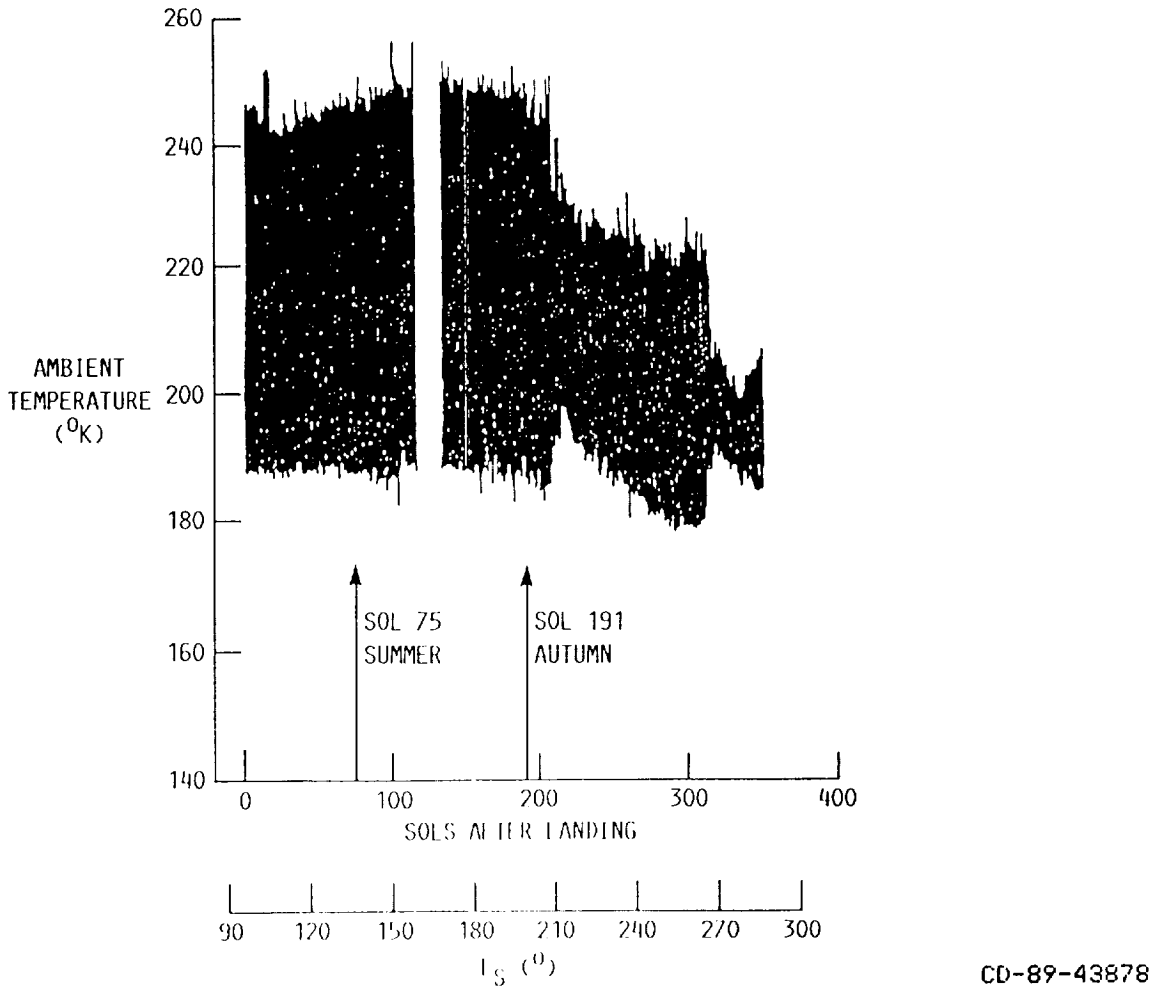

Figure 14: the variation of the ambient temperature at Viking lander VL1 for part of the first year after landing. The top time coordinate is the number of Martian solar days from touchdown; the bottom the seasonal date Ls.

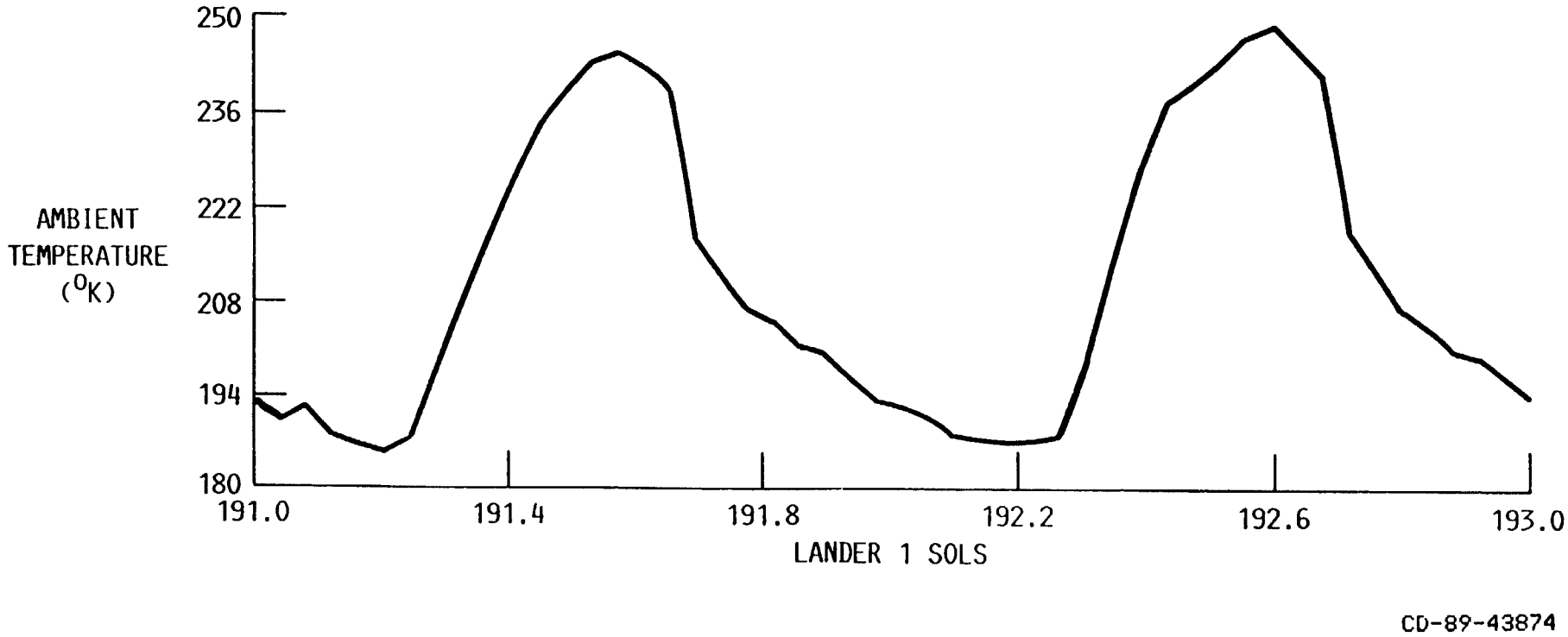

Fig 15: diurnal ambient temperature variation at VL1 for sols 191 and 192 (autumn).

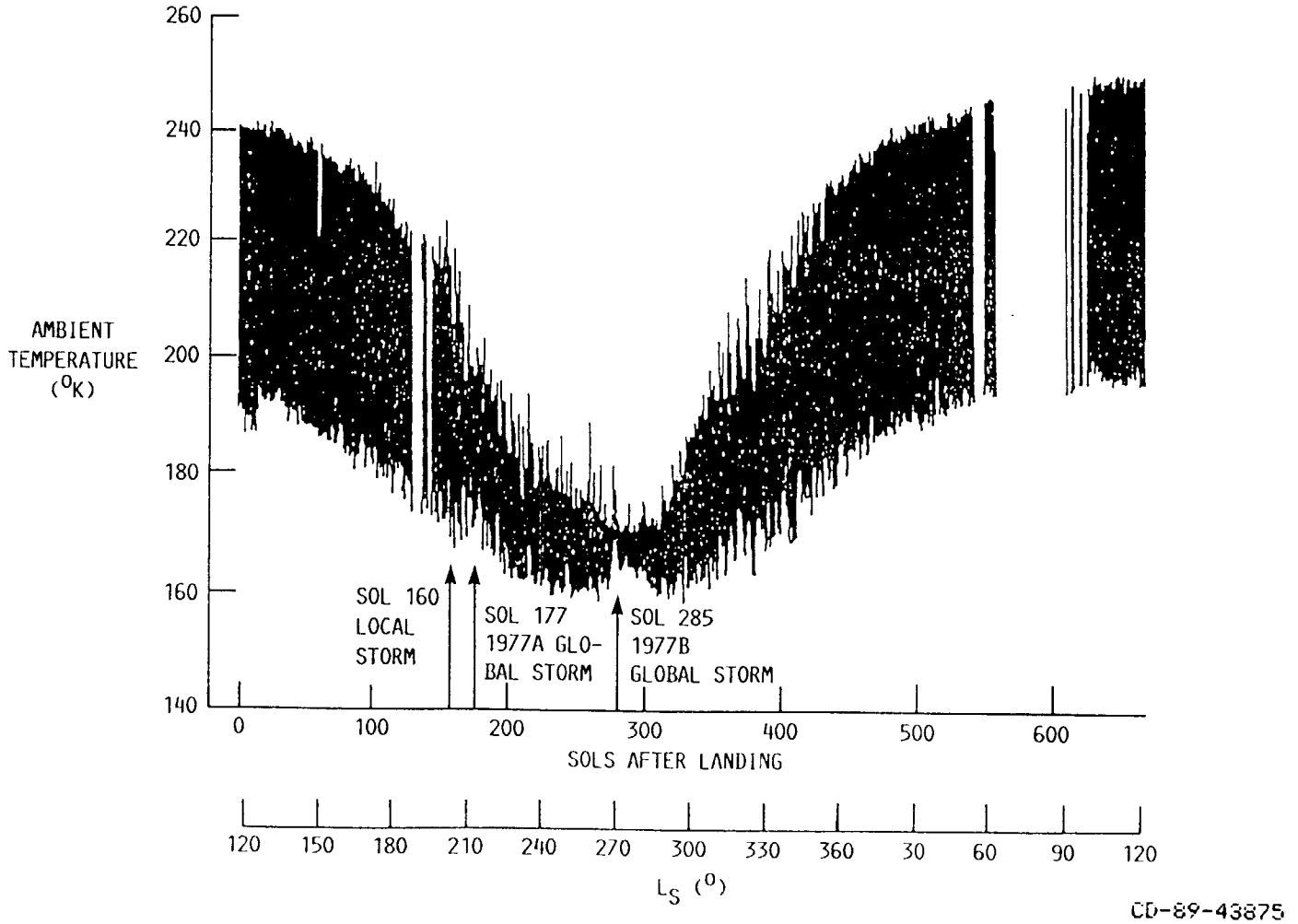

Figure 16: the variation of the ambient temperature at Viking lander VL2 for the first year after landing.

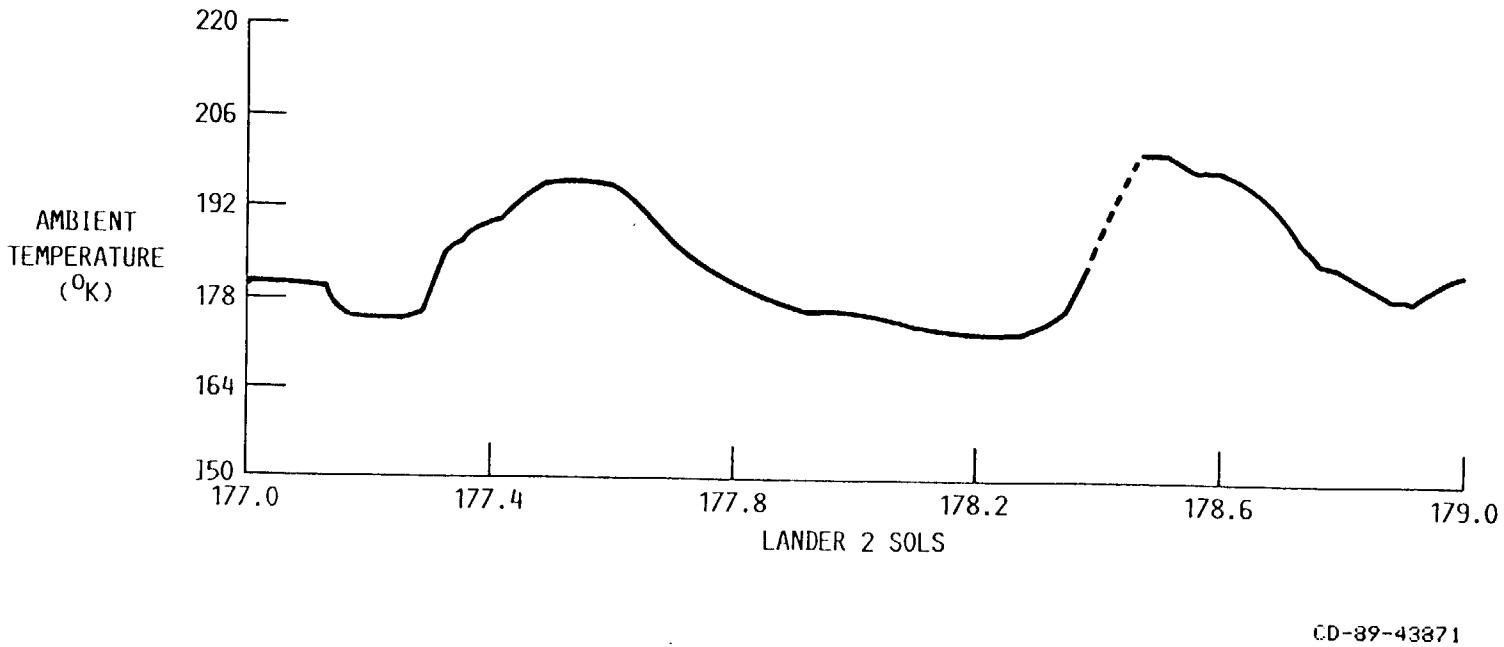

Figure 17: diurnal ambient temperature variation for sols 285 and 286 (1977 B global storm).

Session 4
InP Cells